BEAM TRANSPORT AND STORAGE WITH COLD NEUTRAL ATOMS AND MOLECULES*

P. L. Walstrom and M. D. Di Rosa, LANL, Los Alamos, NM 87545, USA

Abstract

A large class of cold neutral atoms and molecules is subject to magnetic field-gradient forces. In the presence of a field, hyperfine atomic states are split into several Zeeman levels. The slopes of these curves *vs.* field are the effective magnetic moments. By means of optical pumping in a field, Zeeman states of neutral lithium atoms and CaH molecules with effective magnetic moments of nearly ± one Bohr magneton can be selected. Particles in Zeeman states for which the energy increases with field are repelled by increasing fields; particles in states for which the energy decreases with field are attracted to increasing fields. For stable magnetic confinement, field-repelled states are required. Neutral-particle velocities in the present study are on the order of tens to hundreds of m/s and the magnetic fields needed for transport and injection are on the order of in the range of 0.01-1T. Many of the general concepts of charged-particle beam transport carry over into neutral particle spin-force optics, but with important differences. In general, the role of bending dipoles and quadrupoles in charged-particle optics is played by quadrupoles and sextupoles, respectively, in neutral-particle optics. The neutral-particle analog of charge-exchange injection into storage rings is the use of optical pumping to change the state of particles from field-seeking to field-repelled. Preliminary tracking results for two neutral atom/molecule storage ring configurations are presented. It was found that orbit instabilities limit the confinement time in a racetrack-shaped ring with discrete magnetic elements with drift spaces between them; stable behavior was observed in a toroidal ring with a continuous sextupole field. An alternative concept using a linear sextupole or octupole channel with solenoids on the ends is presently being considered.

MAGNETIC-FIELD-GRADIENT FORCES

The effective Hamiltonian for a neutral particle in a particular quantum state subject to field-gradient forces is

$$H(\mathbf{r}) = \frac{1}{2}m\mathbf{v}^2 + mgz + \Delta E_n\left(B(\mathbf{r})\right). \qquad (1)$$

(Note that everywhere in this paper B stands for $|\mathbf{B}|$, the magnitude of the flux-density vector). The gravitational term mgz becomes important for particle velocities on the order of 100 m/s or less. In the case of neutral atoms (here we use ^{7}Li as a model particle) the index n refers to one of the ground-state Zeeman levels (see Fig. 1). Since the slope of the F=2, m_F=2 state of ^{7}Li is constant with field, the effective magnetic moment of this state is constant and very nearly (minus) one Bohr magneton. The effective magnetic moment of the F=1, m_F=1 varies slightly with field at low field but also approaches (plus) one Bohr magneton at higher fields where the slope is constant. If a particle is initially in one of the quantum states, it will stay in that state unless it collides with neutral gas molecules, solid matter, etc., is depolarized by stray radio-frequency fields in resonance with one of the transitions, or is depolarized by passing through a low-field, high-field-gradient region with a sufficiently high velocity (Majorana transition). In order to avoid rf and Majorana transitions, a minimum field ($>$ 10 gauss) is maintained everywhere that a pure quantum state is to be maintained. The criterion for avoiding Majorana transitions with trapped neutral elementary particles with two spin states (e.g., ultra-cold neutrons) is that the Larmor frequency of precession of the magnetic moment of the particle is large in comparison to the fractional rate of change of the magnetic field due to movement through a field gradient (adiabatic limit). In the case of atoms with multiple Zeeman levels, we replace $2|\mu||B/\hbar$ with $\Delta E(B)/\hbar$, where $\Delta E(B)$ is the difference in energy between the stored state and its nearest other Zeeman level:

$$\frac{1}{B}\left|(\mathbf{v}\cdot\nabla)B\right| \ll \frac{\Delta E}{\hbar}. \qquad (2)$$

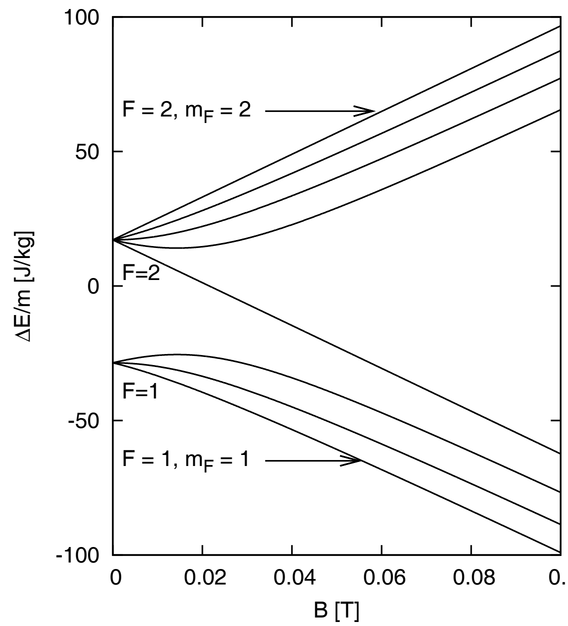

Figure 1: Zeeman splitting of hyperfine ground states of ^{7}Li. The preferred field-repelled state (F=2, m_F=2) and field-seeking state (F=1, m_F=1) are indicated by arrows.

* Work supported in part by the Army Research Office and by the US Department of Energy

The inequality of Eq. 2 is usually easily maintained with the velocities and field gradients of neutral-particle traps, but careful attention must be paid to the detailed 3-D field distributions of real experimental configurations to avoid unwanted field zeroes. Provided that the adiabatic limit is satisfied, the force (combined field-gradient and gravity) becomes

$$\mathbf{F}(\mathbf{r}) = -\frac{dE_n(B)}{dB}\nabla B(\mathbf{r}) - mg\hat{z} \tag{3}$$

In general, magnetic confinement can be divided into two classes: configurations for which particles are everywhere trapped, regardless of the direction of movement (absolute confinement), and configurations for which particles are confined only if the transverse velocity stays within a certain limit. The latter class is analogous to the class of charged-particle accelerators and storage rings, for which in almost all cases the transverse particle momentum is much smaller than the total momentum; if a particle acquires enough transverse momentum it will be lost. In the case of neutral-particle confinement with field-gradient forces, with sufficiently low velocity, it is possible to have absolute confinement. Assuming a particle starts out in a negligibly small magnetic field with velocity v_0 and ignoring gravity, a field-repelled particle in the nth quantum state is absolutely confined if $1/2mv_0^2 < E_n(B) - E_n(0)$. The field for which $1/2mv_0^2 = E_n(B) - E_n(0)$ can be called the turn-around field. For the F=2, m_F=2 state, the turn-around field for v=12.6 m/s is 0.1 T; for 30 m/s, it is 0.56 T.

The magnetic energy $\Delta E_n[B(\mathbf{r})]$ in Eq. 1 plays the role of a classical potential. In accordance with conservation of energy, a field-repelled particle slows down as it enters a high-field region; this causes strong exchange of energy between transverse and longitudinal degrees of freedom. Moreover, the force (see Eq. 3) has a factor of $\nabla B(\mathbf{r})$. Near the axis of a standard multipole magnet, where the field approaches zero, if there is no superimposed solenoidal holding field, the transverse gradient abruptly changes sign; in the case of a quadrupole, it jumps by twice the magnitude of the gradient. Sextupoles are better-behaved because the gradient goes to zero on the axis; away from the fringe-field regions, in an ideal long sextupole the gradient force is radially inward and proportional to the radius. In this sense, there is a partial analogy between quadrupoles in charged-particle transport and sextupoles in neutral-particle transport. In the fringe-field regions, however, the neutral-particle gradient force varies with azimuthal angle even in magnets with pure m-pole symmetry and includes a large longitudinal component. These effects are aggravated by field ripple in non-ideal multipole magnets (e.g. permanent multipole magnets or PMMs constructed with a finite number of wedges), since the field magnitude is differentiated to get the force; in charged-particle transport the force is proportional to the field itself.

TRACKING RESULTS

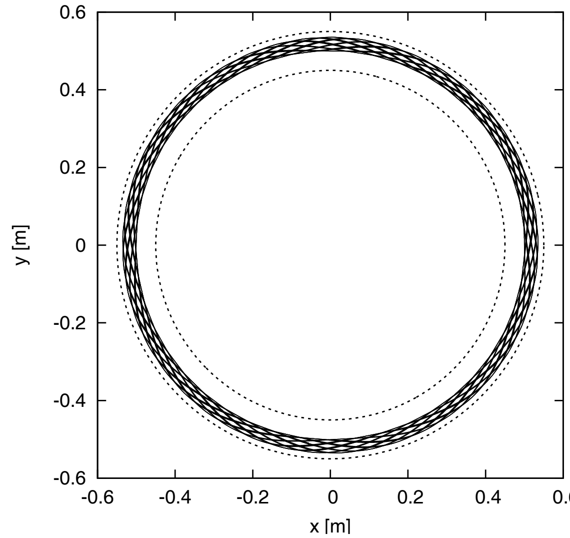

Figure 2: Orbit of a single particle in an azimuthally symmetric toroidal sextupole field. Dashed circles are the intersection of the nominal magnet boundaries with the $x-y$ plane. The particle was tracked for 1.25 s and traveled 100 m.

The first tracking study was carried out with a circular sextupole toroid. By construction, the field was independent of the major azimuthal angle θ. In order to construct a smooth field, 1000 circular current filaments coaxial with the major torus axis were placed on a torus of major radius R =0.5 m and minor radius a=0.05 m. The currents in the filaments were given a $\cos 3\phi$ dependence and an amplitude that gave a maximum field of 1 T. Because of the curvature of the torus, the field was not pure sextupole. The field was evaluated numerically by summing over the contributions of the individual loops, using the usual elliptic-integral expressions. The field values were fit with a double series of the form

$$B_r(\rho, \phi) \approx \sum_{n=1}^{6}\sum_{k=n}^{6} A_{nk}\rho^k \sin n\phi \tag{4}$$

$$B_z(\rho, \phi) \approx \sum_{n=0}^{6}\sum_{k=n}^{6} B_{nk}\rho^k \cos n\phi. \tag{5}$$

In Eqs. 4 and 5, r and z are the distances from the major axis and midplane, respectively, and ρ and ϕ polar coordinates around the minor axis. The best fit was obtained by shifting the minor axis of the fit to a radius slightly smaller than the major radius R of the torus. Fields computed with the fit agreed with fields computed with the loops to better than one part in 10^7 and field derivatives to better than one part in 10^5. A small toroidal holding field, $B_\theta = B_0R/r$, everywhere perpendicular to the sextupole field, was added to avoid a field zero near the minor axis. The equations of motion (see Eq. 3) were numerically integrated in Cartesian coordinates by a symplectic leapfrog routine. It was found that if a particle was not lost in the first revolution, motion was stable and quasi-periodic and it would stay in the torus essentially indefinitely (within the limits of numerical error). Figure 2 is a plot of the orbit of a typical stored particle. As expected, the average radius is shifted outward from the torus minor radius. Also, when tracking ensembles of particles with a finite spread of initial 6-D phase-space coordinates for a fixed time larger than several revolution times, it was found that final positions of the particles were spread out in θ more or less uniformly around the ring. A second tracking study was carried

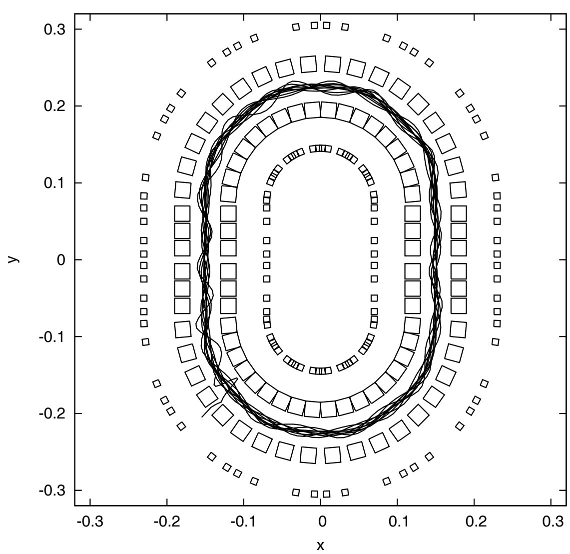

Figure 3: Orbit of a single particle in a discrete-sextupole racetrack ring. The inner rectangles are the intersections of the sextupoles with the $x-y$ plane and the outer rectangles indicate solenoids. In this case, the particle was lost after 0.4 s and 9 revolutions.

out with a racetrack-shaped array of discrete permanent-magnet sextupoles and solenoids (see Fig. 3). The PM sextupoles were modeled by a finite number of trapezoidal segments. In modeling standard permanent-multipole magnets (PMMs) each segment has a constant volume magnetization of $B_{\rm rem}$ of 1.1 T. With the standard Halbach rotation, $M_x = B_{\rm rem} \sin[(m+1)\bar{\phi}$, $M_y = -B_{\rm rem} \cos[(m+1)\bar{\phi}$, where $\bar{\phi}$ is the mean azimuthal angle of the segment. The field and field derivatives from the magnet segments was modeled by summing over analytic expressions for the rectangular faces with constant surface magnetic-charge densities $\sigma = \mathbf{M} \cdot \mathbf{N}$, where $\mathbf{N}$ is the unit outward normal vector to a face. The field contributions from the solenoids were modeled with elliptic-integral expressions. For the tracking shown in Fig. 3, the sextupoles had two segments/pole. Typical ^{7}Li velocities were 30 m/s.

A first series of tracking runs with standard PM sextupoles showed large instabilities, with particles with initial distances from the magnet centers of one-half of the magnet radius being lost in a quarter turn; particles released on the magnet axis with small transverse velocities traveled farther, but exhibited exponentially increasing transverse oscillations until they were lost. Some improvement in stability was achieved by modulating the magnetization strength in an *ad hoc* fashion to lower the sextupole field at the inner radius of the bends. This was done by setting $|\mathbf{M}|(\phi) = 1/2[1+f+(1\text{-}f)\cos\phi]B_{\rm rem}$, with $0 < f < 1$. In practice, such modulation would be better achieved by using PMMs with a wedge-shaped projection on the $x-y$ plane (racetrack midplane) to reduce the gaps on the outside of the bends, but an analytic model for such elements is not yet available. The longest trajectories (some particles were tracked for up to 0.5 s) were achieved with f =0.4 to 0.6. Fig. 3 had magnets with $f = 0.5$. However, unlike the case of the smooth sextupole torus, no stable trajectories were found for the discrete-sextupole racetrack even with the modifications.

In order to study the effect of curvature on sextupole channels, tracking studies were done with very long straight channels (30 m) of equally spaced discrete finite PM sextupoles with small gaps between them, with added holding-field solenoids. The unit cell was essentially that of the straight sections of the racetrack of Fig. 3. No instabilities were observed in these channels. The above results only suggest that no stable racetrack configuration with significant gaps between magnets exists; more studies, especially with wedge PMMs in the bends are needed. For velocities less than about 20 m/s, a continuous racetrack of PM sextupoles with no gaps (using wedge PM sextupoles in the bends) would provide absolute confinement even if the velocity were to be completely in the transverse direction, since the sextupole field near the inner radius of the sextupoles would be greater than the turn-around field. However, such a configuration would not allow for particle injection. Adding a gap for injection would open up the possibility of instabilities due to the gap.

ALTERNATIVE CONCEPT

If tracking simulations with racetracks, especially with an added injection chicane, continue to exhibit unacceptable instabilities, an alternative is to use a continuous (no gaps) linear sextupole or octupole channel with barrier solenoids at the ends. The design would be based on absolute confinement. This configuration was proposed for confinement of ultra-cold neutrons [1]. Injection would be done through the bore of one of the solenoids with particles in a field-seeking state. After the injected particles have passed through the peak of the barrier field and have reached a region with a field less than one-half of the peak value, the particles are optically pumped to a field-repelled state and are absolutely confined.

REFERENCES

[1] K.K.H. Leung and O. Zimmer, Nucl. Inst. Meth. A, Vol. 611, Issues 2-3, 1-11 Dec. 2009, p. 181.

ISBN 978-3-95450-115-1